[7]Torenbeek, E., *Synthesis of Subsonic Airplane Design*, Delft Univ. Press, Kluwer Academic, Norwell, MA, 1982, pp. 167–170, 263–294, 445–465, 487–556.
[8]Raymer, D. P., *Aircraft Design: A Conceptual Approach*, AIAA Education Series, AIAA, Washington, DC, 1989, pp. 391–405.
[9]Crossley, W. A., and Laananen, D. H., "Conceptual Design of Helicopters via Genetic Algorithm," *Journal of Aircraft*, Vol. 33, No. 6, 1996, pp. 1062–1070.
[10]Crispin, Y., "Adaptive Conceptual Optimization of General Aviation Aircraft," AIAA Paper 92-4195, Aug. 1992.
[11]Crispin, Y., "Aircraft Conceptual Optimization using Simulated Evolution," AIAA Paper 94-0092, Jan. 1994.
[12]Bramlette, M. F., and Cusic, R., "A Comparative Evaluation of Search Methods Applied to Parametric Design of Aircraft," *Proceedings of the 3rd International Conference on Genetic Algorithms*, Morgan Kaufmann, San Mateo, CA, 1989, pp. 213–238.
[13]Roth, G. L., and Crossley, W. A., "Conceptual Design of a Commercial Transport Aircraft Using a Genetic Algorithm-Based Approach," AIAA Paper 98-4934, Sept. 1998.
[14]Roskam, J., *Airplane Design—Part VIII*, Roskam Aviation and Engineering Corp., Kansas, 1988, Chap. 5, pp. 80–109.
[15]Goldberg, D. E., *Genetic Algorithms in Search, Optimization and Machine Learning*, Addison Wesley Longman, Reading, MA, 1989, pp. 59–88.

Numerical Evaluation of Airfoil Friction Drag

Giovanni Lombardi,* Maria Vittoria Salvetti,† and Dario Pinelli‡
University of Pisa, 56126 Pisa, Italy

Introduction

THE prediction of friction drag is of significant importance in the design of aerodynamic configurations, especially in aircraft design. Unfortunately, this is traditionally a difficult task, both experimentally and numerically. In experiments, it is difficult to reproduce all of the features of the physical problem, for example, the Reynolds number. Moreover, problems arise due to interference effects, in particular with the model support, and due to the difficulty in measuring quantities that are small compared to the others involved in the tests. From the numerical point of view, in the past only potential flow solvers were available. Thus, predictions were substantially limited to the induced drag, and only attached flow conditions in subsonic or supersonic regimes could be analyzed.

The use of a boundary-layer model has been a powerful tool, for friction drag prediction, but it is limited to attached flows. The increase in computing performance has lead to the possibility of simulating more complex flows. At present, several commercial codes are available that discretize laminar and Reynolds-averaged Navier–Stokes equations (RANS). These codes are widely used to predict the pressure loads acting on bodies of different shapes and also on aerodynamic configurations. Examples of such applications can be found, for instance, in Refs. 1 and 2.

In principle, the RANS codes are able to predict both the pressure and friction components of drag. This approach seems very attractive because numerical analysis requires lower cost and less time to obtain results than experimental tests. However, although the capabilities of RANS codes are well stated for the evaluation of pressure distributions,[1] many problems still exist for the evaluation of the friction drag, which appears to be very sensitive to near-wall grid resolution and to the employed turbulence model.

In this Note the capabilities of a Navier–Stokes solver to predict the friction drag over an airfoil are studied. In particular, the sensitivity to the grid resolution and to different RANS closure models is investigated for three different Reynolds numbers.

Numerical Methods

The commercial code FLUENT 5.0 has been used for the numerical solution of RANS equations. Different turbulence models are available in the code. In particular, the standard k–ε,[3] Renormalization Group (RNG) k–ε,[4] and Reynolds stress[5] models are used in the present study. The numerical method is based on a finite volume formulation applicable to structured or unstructured solution-adaptive grids. The numerical inviscid fluxes are evaluated by Roe's flux-difference splitting. A second-order spatial accuracy is obtained by a Taylor series expansion in the evaluation of the variables at the cell faces. Steady solutions are obtained by time marching the equations with an explicit, multistage, Runge–Kutta scheme with multigrid convergence acceleration.

Unfortunately, no experimental results are available for the friction drag. Therefore, the results are compared with those obtained by a boundary-layer solution, coupled with a potential solver. Clearly, this limits the analysis to subsonic flows and low angles of attack. However, this is a necessary first step in the assessment of the Navier–Stokes solver capabilities and may also give indications as to the computational resources needed for friction drag prediction on more complex configurations of engineering interest.

For boundary-layer evaluation, the code BLOWS[6] was used. This code is based on the Thwaites method for the simulation of the laminar boundary layer and on the Head method for the turbulent one. The code is able to predict the transition from laminar to turbulent flow.

Results

The analysis has been carried out by simulating the flow around the NACA 0012 airfoil, at 0-degree angle of attack, for three different values of the Reynolds number.

The results of the code BLOWS, in terms of total drag, are compared with the experimental data from Ref. 7 in Table 1. The comparison shows that the code is able to correctly predict the drag in the analyzed conditions, and, therefore, the results for the friction drag can be assumed as a reference.

The values of the friction coefficient obtained by the RANS solver are reported in Table 2 for different grid resolutions. The results are obtained at a Reynolds number of 3×10^6 using the standard k–ε turbulence model. In all of the cases, the grid is unstructured, and the near-wall resolution is increased by prescribing the maximum allowable distance from the body of the first cell centroid, in terms of wall units, $y^+ = u_\tau y/\nu$, where u_τ is the friction velocity, y is the physical distance of the first centroid from the wall, and ν is the kinematic viscosity. Because a logarithmic wall law is used in FLUENT to compute the friction coefficient, the first grid cell near the body should be in the logarithmic region, that is, $y^+ > 30$. From Table 2, it can be seen that an acceptable convergence of the computed value of the friction drag coefficient is reached only for $y^+ \leq 38$. For $y^+ \leq 38$, the chord distribution of the local friction drag

Table 1 Comparison between experimental data and BLOWS code results[a]

Reynolds	$C_{d\,\text{total}} \times 10^3$ (Ref. 7)	$C_{d\,\text{total}} \times 10^3$	$C_F \times 10^3$
3×10^6	6.0	6.228	5.340
6×10^6	6.0	6.173	5.040
9×10^6	6.0	6.208	5.080

[a]C_d and C_F are the airfoil drag and friction coefficients, respectively.

Received 18 October 1999; revision received 30 November 1999; accepted for publication 2 December 1999.

*Assistant Professor, Department of Aerospace Engineering, Via Diotisalvi 2. Member AIAA.
†Assistant Professor, Department of Aerospace Engineering, Via Diotisalvi 2.
‡Graduate Student, Department of Aerospace Engineering, Via Diotisalvi 2.

Table 2 Friction coefficients for different grid resolution (k–ε model), Reynolds number = 3×10^6

y^+	Wall cells	Total cells	$C_F \times 10^3$
2,390	50	1,378	7.527
1,191	100	2,010	8.248
591	200	3,060	7.922
391	300	4,164	8.023
295	400	5,114	8.072
144	800	9,376	7.974
93	1,200	13,790	7.797
69	1,600	17,614	7.751
54	2,000	21,732	7.566
45	2,400	26,046	7.670
38	2,800	30,056	7.486
35	3,200	33,946	7.321
33	3,600	37,732	7.325
27	4,000	37,916	7.300
BLOWS	——	——	5.340
BLOWS fully turbulent	——	——	6.349

Table 3 Friction coefficients for different grid resolutions (k–ε model), Reynolds number = 6×10^6

y^+	Wall cells	Total cells	$C_F \times 10^3$
1,117	200	3,600	6.936
557	400	5,114	7.078
72	2,800	30,056	6.607
63	3,200	33,946	6.455
64	3,600	37,916	6.464
52	4,000	37,732	6.462
BLOWS	——	——	5.040
BLOWS fully turbulent	——	——	5.665

Table 4 Friction coefficients for different grid resolutions (k–ε model), Reynolds number = 9×10^6

y^+	Wall cells	Total cells	$C_F \times 10^3$
104	2,800	30,056	6.134
91	3,200	33,946	5.944
95	3,600	37,916	5.999
76	4,000	37,732	6.012
BLOWS	——	——	5.080
BLOWS fully turbulent	——	——	5.298

coefficient is also independent of the grid resolution (not shown here for sake of brevity).

The same analysis also has been carried out at Reynolds numbers of 6×10^6 and 9×10^6 (Tables 3 and 4). As the Reynolds number increases, grid independence is reached with a higher value of y^+ ($y^+ \cong 60$ at $Re = 6 \times 10^6$ and $y^+ \cong 90$ at $Re = 9 \times 10^6$), but the number of grid cells required is approximately the same for all of the Reynolds numbers.

Similar results have been obtained for the RNG k–ε and the Reynolds-stress closure models and with an hybrid grid, structured near the wall.

This analysis shows that, even in this simple test case, a large number of cells is needed at the wall to reach grid independence of the calculated friction drag. It would be hard, if not impossible, to reach such a resolution in three-dimensional calculations.

Once grid independence has been reached, the C_F values obtained from the RANS simulations are significantly larger than those given by the potential/boundary-layer solver (Table 1). As the Reynolds number increases, the overestimate appears to decrease (35% at $Re = 3 \times 10^6$ with $y^+ = 35$ and 18% at $Re = 9 \times 10^6$ with $y^+ = 95$). This discrepancy is because, in the RANS calculations with the k–ε turbulence model, the whole boundary layer is considered turbulent, whereas the criterion used in BLOWS predicts the transition at $x/c = 0.38$, 0.33, and 0.26 for $Re = 3 \times 10^6$, 6×10^6, and 9×10^6, respectively. Indeed, if the potential/boundary-layer simulations are carried out with an imposed fully turbulent boundary layer, the values of C_F increase and become more similar to those obtained with the RANS solver (Tables 2–4).

Table 5 Friction coefficients for different turbulence models

Turbulence model	y^+	$C_F \times 10^3$
Standard k–ε	38	7.486
RNG k–ε	49	6.272
Reynolds stress	38	6.792
BLOWS	——	5.340
BLOWS (fully turbulent)	——	6.349

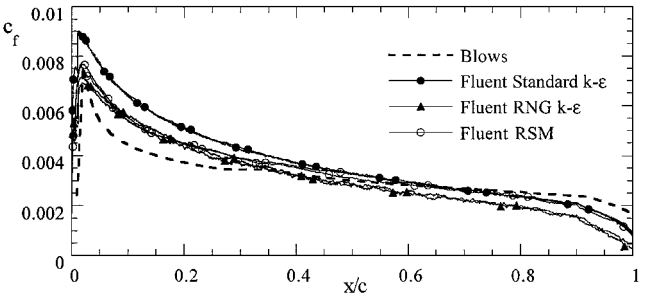

a) Comparison between different turbulence models

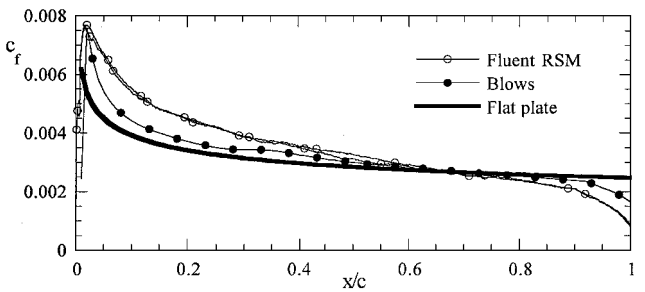

b) Comparison with the flat plate distribution

Fig. 1 Local friction coefficient along the chord at Reynolds number 3×10^6.

Because, from the preceding analysis, the simulation at $Re = 3 \times 10^6$ appears to be the most critical for the RANS solver, the sensitivity to the turbulence closure model has been investigated at this Reynolds number. In Table 5 the values of C_F obtained with the three turbulence models are reported, together with the values given by the BLOWS code.

The influence of the turbulence model is clearly significant, with a difference between the highest (given by the standard k–ε model) and the lowest (RNG k–ε) values of C_F of about 20%. In all of the RANS simulations, the total friction drag coefficient is overestimated in comparison to the value given by the potential code when boundary-layer transition is considered. A quite good agreement is observed between the C_F obtained with the RNG k–ε and the Reynolds-stress models and that given by the BLOWS code with a fully turbulent boundary layer. This behavior can be better understood by comparing the chord distributions of the local friction coefficient c_f (Fig. 1a). It is evident that the standard k–ε model overestimates the peak near the leading edge. This is probably caused by the overestimation of the value of k in this zone, typical of this model of closure.[1] The other turbulence models show a better agreement in the leading-edge zone, but a lower gradient after the peak. In the rear part of the airfoil, the RNG k–ε model shows an underestimate of the friction drag as compared with the BLOWS code. Thus, the

integral value obtained with this method results very close to that obtained with the potential/boundary-layer simulation. However, it seems that the better prediction of the local behavior of the friction drag is obtained with the Reynolds-stress closure method. Note that for the RANS simulations the values of c_f obtained on both the upper and lower airfoil surfaces are reported. Because symmetry is not perfect, because of discretization errors, two slightly different lines can be distinguished.

In Fig. 1b, the local friction drag coefficient distributions obtained by the RANS and the boundary-layer methods are compared to the theoretical results for the flat plate. In both cases, the friction drag on the profile is higher than that on the flat plate in the leading-edge zone, although it is lower near the trailing edge. This behavior is consistent with the effects of the chordwise pressure gradient. Because the pressure distributions are practically the same in all of the simulations, the Reynolds-stress closure method predicts a larger variation of the local coefficient c_f with the pressure gradient than the potential/boundary-layer simulation. However, it is expected that RANS simulations give a better representation of the effects of the pressure gradient than the boundary-layer method; thus, it is not clear which solution is the most accurate in the leading-edge region.

The computations were carried out on a Pentium III 500-MHz XION processor, with 512 MB RAM. The computing time for the case with 34,000 total cells was about 70 min for the standard k–ε closure method, 110 min for the RNG k–ε closure method, and 150 min for the Reynolds-stress closure method (with a few seconds for the potential/boundary-layer simulations). Therefore, the Reynolds-stress closure method appears significantly more time consuming. In general, the RANS calculations seem to require computational resources, both memory and computing time, which would become prohibitive in three-dimensional calculations.

Conclusions

The capabilities of a solver of the RANS equations in predicting the friction drag over an airfoil have been investigated through comparison with the values given by a coupled potential/boundary-layer method, for different Reynolds numbers.

Preliminarily, the near-wall grid resolution required to obtain the grid independence of the friction drag in the RANS calculations has been assessed. It appears that, for all of the considered Reynolds numbers, a large amount of computational points is required, which would lead to an unaffordable mesh size in three-dimensional simulations.

Even on these highly refined grids, the value of the global C_F is overestimated by all of the turbulence models because they are not able to predict the boundary-layer transition. If comparison is made with the value given by the potential code coupled with a fully turbulent boundary layer, satisfactory agreement is obtained with the RNG k–ε and the Reynolds-stress closure models. The best global agreement is given by the RNG k–ε model. However, from the analysis of the chord distribution of the local c_f, it appears that this is due to compensation between an overestimate near the leading edge and an underestimation at the trailing edge.

The best local agreement is obtained, as expected, with the Reynolds-stress model; the only significant discrepancy with the BLOWS results is a less steep decrease of the c_f near the leading edge. Because the pressure distribution is almost identical, it appears that the RANS simulation with this closure models predicts larger variations of the friction coefficient with the pressure gradient. Because the boundary-layer solvers are not well suited for flows with high-pressure gradients, it is not clear whether the value of c_f obtained by potential/boundary-layer simulation is indeed more accurate in the region near the leading edge.

Finally, the RANS simulations require in general large computational time, and this increases significantly with the accuracy of the turbulence closure model. Thus, this analysis indicates that an accurate prediction of the friction drag around complex aeronautical configurations by RANS methods remains an extremely difficult task with the present computer capabilities.

References

[1] Lombardi, G., Morelli, M., and Salvetti, M. V., "Appraisal of Numerical Methods in Predicting the Aerodynamics of Forward Sweep Wings," *Journal of Aircraft*, Vol. 35, No. 4, 1998, pp. 561–568.

[2] Lombardi, G., Salvetti, M. V., Talamelli, A., "Shock-Wave/Boundary-Layer Interaction in Transonic Flow Around a Forward-Swept Wing," AIAA Paper 97-1838, June 1997.

[3] Launder, B. E., and Spalding, D. B., *Lectures in Mathematical Models of Turbulence*, Academic, London, 1972.

[4] Yakhot, V., and Orszag, S. A., "Renormalization Group Analysis of Turbulence: I. Basic Theory," *Journal of Scientific Computing*, Vol. 1, No. 1, 1986, pp. 1–51.

[5] Launder, B. E., "Second-Moment Closure: Present . . . and Future?," *International Journal of Heat Fluid Flow*, Vol. 10, No. 4, 1989, pp. 282–300.

[6] Baricci, A., "Procedura di Calcolo dell'Interazione Strato Limite-Flusso Potenziale su Profili Alari," Tesi di Laurea in Ingegneria Aeronautica, Univ. of Pisa, Italy, Nov. 1989.

[7] Abbott, I. H., and Von Doenhoff, A., *Theory of Wing Section*, Dover, New York, 1949.

Boundary-Layer Transition, Separation, and Reattachment on an Oscillating Airfoil

T. Lee* and G. Petrakis†
McGill University, Montreal, Quebec H3A 2K6, Canada
and
F. Mokhtarian‡ and F. Kafyeke§
Bombardier Aerospace,
Montreal, Quebec H3C 3G9, Canada

Introduction

CONSIDERABLE effort[1–10] has been made to investigate the flow structure around an airfoil with unsteady motions to advance the understanding of the unsteady flows developed on aerodynamic objects in unsteady motion and to continue the development and validation of predictive methods. An excellent review on unsteady aerodynamics is given by McCroskey.[11] Recently, the spatial–temporal progression of the boundary-layer events (i.e., the locations of leading-edge stagnation, transition, separation, and reattachment points) that occurred on a sinusoidally oscillated NACA 0012 airfoil model was identified nonintrusively by Lee and Basu[12] using multiple hot-film sensor arrays. However, due to the limitations of their experimental setup, only low-frequency/small-amplitude oscillations were investigated. In the present experiment, the effects of large oscillation frequency $0.05 \leq \kappa (= \pi f_0 C / U_\infty$, where f_0 is the oscillation frequency, C is the chord length, and U_∞ is the freestream velocity) ≤ 0.30 and amplitude (both within, through, and well beyond the static-stall angle of attack α_{ss}) on the unsteady boundary layer developed on an NACA 0012 airfoil model oscillated sinusoidally were examined using multiple hot-film sensor arrays. The hot-film measurements were then used to postulate the mechanisms responsible for these boundary-layer events.

Experimental Methods and Apparatus

The experiments were performed in a 60 cm × 90 cm × 1.8 m low-speed wind tunnel. An NACA 0012 airfoil, fabricated from

Received 14 May 1999; revision received 3 August 1999; accepted for publication 30 August 1999.

*Assistant Professor, Department of Mechanical Engineering.
†Graduate Student, Department of Mechanical Engineering.
‡Section Chief, Advanced Aerodynamics.
§Manager, Advanced Aerodynamics.